Available online at www.sciencedirect.com
ScienceDirect
Bioorganic & Medicinal Chemistry Letters 18 (2008) 1340–1345
Bioorganic & Medicinal Chemistry Letters

Discovery of novel inhibitors of 11β-hydroxysteroid dehydrogenase type 1 by docking and pharmacophore modeling

Huaiyu Yang,[a] Wei Dou,[b] Jing Lou,[b] Ying Leng[b,*] and Jianhua Shen[a,c,*]

[a]*Drug Discovery and Design Center, State Key Laboratory of Drug Research, Shanghai Institute of Materia Medica, Shanghai Institutes for Biological Science and the Graduate School, Chinese Academy of Sciences, 555 Zuchongzhi Road, Shanghai 201203, China*
[b]*Shanghai Institute of Materia Medica, Chinese Academy of Sciences, China*
[c]*School of Pharmacy, East China University of Science and Technology, Shanghai 200237, China*

Received 27 August 2007; revised 31 December 2007; accepted 5 January 2008
Available online 11 January 2008

Abstract—11β-hydroxysteroid dehydrogenase type 1 (11β-HSD1) is a potential target for treatment of diabetes and metabolic syndrome. Docking and pharmacophore modeling have been used to discover novel inhibitors of 11β-HSD1. Several compounds, with large structural diversity and good potency against 11β-HSD1, have been found and their potency was determined by the enzyme assay. New scaffolds of 11β-HSD1 inhibitors are also reported.

Glucocorticoids regulate hepatic gluconeogenesis through activation of glucocorticoid receptor. Glucocorticoids are notably excess in Cushing's syndrome, which causes metabolic abnormalities, such as visceral obesity, impaired glucose tolerance, atherosclerosis, dyslipidemia, and hyperglycemia.[1,2] Normalization of glucocorticoid level can reverse the features of metabolic syndrome.[3] Thus, suppression of glucocorticoid action might be a potential therapy for metabolic syndrome. The principal glucocorticoid is cortisol (hydrocortisone). Cortisol concentration in target tissues is modulated by tissue-specific enzymes: 11β-hydroxysteroid dehydrogenase type 1 (11β-HSD1) and type 2 (11β-HSD2). 11β-HSD1, predominantly expressed in liver and adipose tissue, catalyzes the conversion of inactive cortisone into glucocorticoid receptor-active cortisol; while 11β-HSD2, expressed mainly in the kidney, catalyzes the reverse reaction. It was reported that 11β-HSD1 knockout mice show reduced weight gain on a high-fat diet, improved glucose tolerance and insulin sensitivity, and a decreased hepatic gluconeogenic response to fasting.[4] In contrast, animals with elevated adipose 11β-HSD1 expression develop metabolic syndrome-like phenotypes, such as central obesity and insulin resistance.[5] In addition, transgenic mice with increased 11β-HSD2 expression in adipose tissue resist weight gain on high-fat diet, which is associated with increased energy expenditure and improved glucose tolerance as well as insulin sensitivity.[6] These data suggest that 11β-HSD1 could be a potential target for treatment of diabetes and metabolic syndrome.[7,8]

Numerous efforts have been made toward 11β-HSD1 and many inhibitors have been reported.[9–11] In the present study, molecular docking and pharmacophore-based database search are used to discover new 11β-HSD1 inhibitors. When our work was in progress, two in silico studies on 11β-HSD1 were reported.[12,13] Miguet et al. used a homology model for docking to identify 11β-HSD1 inhibitors.[12] However, in our study, crystallographic structure rather than homology model is applied for docking. Schuster et al. used pharmacophore modeling method to discover both selective and nonselective 11β-HSD1 inhibitors.[13] Differently, we only choose different compounds with high bioactivity, selectivity, and structural diversity to construct selective pharmacophore model. Moreover, we have combined molecular docking with pharmacophore-based database search. The 3000 compounds used in pharmacophore-based database search were selected by docking. Totally, we selected 162 compounds by molecular docking and pharmacophore-based database search. Among them,

Keywords: 11β-HSD1; 11β-HSD2; Inhibitor; Docking; Pharmacophore.
* Corresponding authors. Tel.: +86 21 50806600x1203; fax: +86 21 50807088; e-mail addresses: yleng@mail.shcnc.ac.cn; jhshen@mail.shcnc.ac.cn

0960-894X/$ - see front matter © 2008 Elsevier Ltd. All rights reserved.
doi:10.1016/j.bmcl.2008.01.020

Table 1. Inhibition of human 11β-HSD1[a]

Compound	IC_{50} (μM)
1	4.58
2	0.26
3	14.60
4	1.95
5	0.77
6	5.87
7	6.28
10	1.85
11	3.74
12	3.57
13	0.69
Enoxolone	11.78[b]

[a] Values are averages of three determinations and deviation from the average is <10% of the average value.
[b] nM.

121 compounds were purchased and evaluated by enzyme assay. Several compounds with large structural diversity show high inhibition against 11β-HSD1. Inhibition of human and mouse 11β-HSD1 and 11β-HSD2 enzymatic activity was determined by scintillation proximity assay (SPA) using microsomes containing 11β-HSD1 or 11β-HSD2.[14] Meanwhile, enoxolone was tested as the positive control.

When the present work started, five released crystal structures of human 11β-HSD1 complex were available (PDB entries: 1XU9, 1XU7, 2BEL, 1Y5M, and 1Y5R).[15,16] Two dimers, 1Y5M and 1Y5R, were not chosen as the model for docking, because the ligands in the binding pockets of 1Y5M are octanes and the limitation of 1Y5R is its low resolution. In 2BEL there are two dimers in the asymmetric unit. 1XU9 and 1XU7 are tetramers. Because of its highest resolution, 1XU9 was

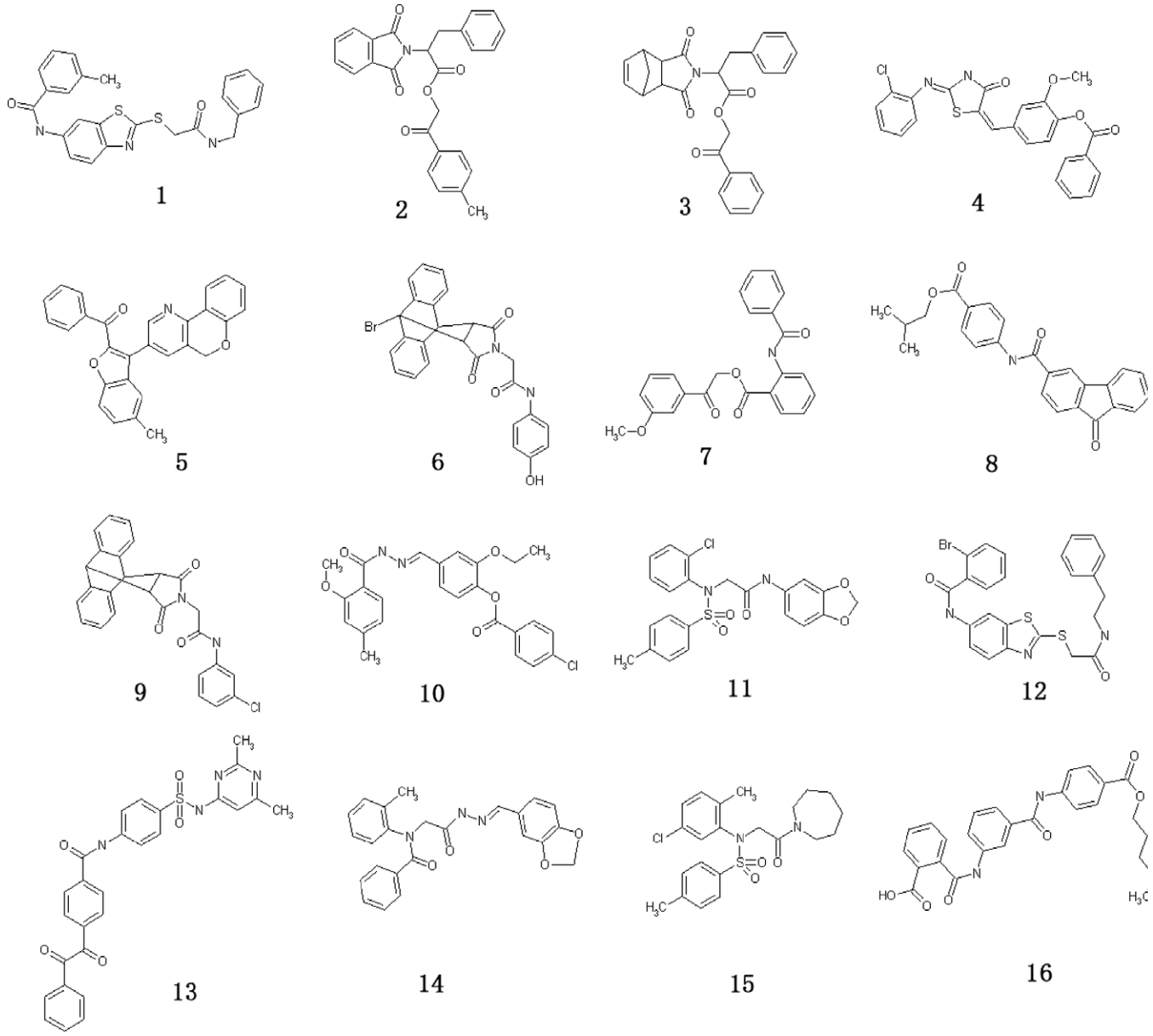

Figure 1. Structures of the active compounds.

chosen as the model for docking. Residues within a radius of 5 Å around the ligand were used to construct the grids for docking screening. The SPECS database containing the structural information of 190,000 chemicals (http://www.specs.net) was adopted for virtual screening. The program DOCK4.0[17,18] was employed for the primary screening. During the docking calculations, Kollman-all-atom charges[19] were assigned to the protein, and Gasteiger–Hückel charges[20] were assigned to the small molecules. Conformational flexibility of the small molecules was implemented in the docking search. The ligand–receptor binding energy was approximately set to be the sum of the van der Waals and electrostatic interaction energies. After an initial evaluation of the orientation and scoring, a grid-based minimization was carried out for the ligand to locate the nearest local energy minimum within the receptor binding site. Position and conformation of each docked molecule were optimized by using the single-anchor search and torsion minimization method. The 3000 compounds with the highest score resulting from DOCK4.0 search were selected for the second round docking by using the Glide program (Schrödinger, LLC, New York, NY, 2005). Receptor was prepared by using the Protein Preparation and Grid Preparation tools in the Schrödinger Maestro interface. The default settings were adopted for the cutoff, neutralization, scaling, dimensions of the binding pocket used for grid preparation, and treatment of cofactor. Rigid docking was applied. Subsequently, a chemistry space filter for scoring druglikeness[21] developed by our group was used to remove the nondruglike structures of the 300 compounds with highest *G* scores.

Then, 62 compounds were selected for purchase but only 39 compounds were purchased because the other 23 compounds were out of stock. These compounds were evaluated by the enzyme assay for their inhibition of the human and mouse 11β-HSD1. At the concentration of 10 μM, their inhibition against human 11β-HSD1 varies from 0% to 91.2%. The IC_{50} values of seven compounds with high inhibition (compounds **1**–**7**, Table 1 and Fig. 1) were determined. Three of the 39 compounds showed high inhibition of mouse 11β-HSD1 (compounds **2**, **8**, and **9**, Table 2 and Fig. 1). Compounds **8** and **9** inhibited mouse 11β-HSD1 with IC_{50} values of 3.60 and 12.49 μM, respectively. Compound **2** showed ~60% inhibition of mouse 11β-HSD1 at the concentration of 10 μM. However, dose-dependent inhibition was not observed in subsequent study. We were not able to get the IC_{50} values of compound **2**. Interestingly, compounds showed different inhibition of human 11β-HSD1 and mouse 11β-HSD1. It might be due to the variability of the active site of 11β-HSD1 in two species[22] since we used crystal structure of the human 11β-HSD1 rather than the mouse 11β-HSD1 as the starting model for docking. In addition, the general hydrogen-bond interaction models of compounds **1**–**7** with the human 11β-HSD1 were studied. As shown in Figure 2B, compound **6** forms a hydrogen bond with the residue Thr124, while compounds **1**, **3**, **6**, and **7** form hydrogen bonds with the residue Tyr183. The ligand complexed in the crystallographic structure

Table 2. Inhibition of mouse 11β-HSD1[a]

Compound	IC_{50} (μM)
8	3.60
9	12.49
12	2.09
13	0.48
15	6.10
16	2.36
Enoxolone	10.58[b]

[a] Values are averages of three determinations and deviation from the average is <10% of the average value.
[b] nM.

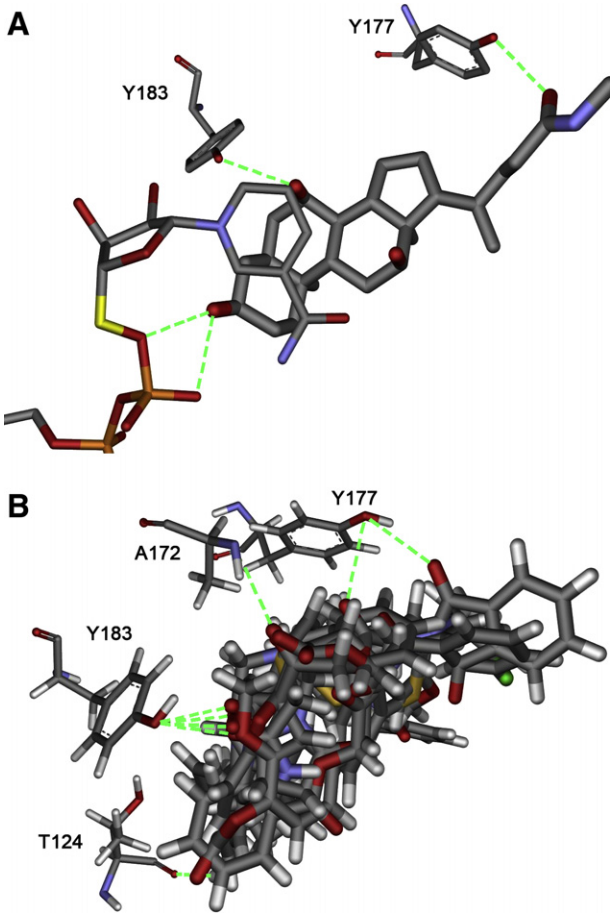

Figure 2. Representatives for the hydrogen-bond interaction models. (A) Hydrogen-bond interactions between the complexed ligand and other atoms in 1XU9.pdb. (B) Hydrogen-bond interactions of compounds **1**–**7** with human 11β-HSD1. The broken lines in green represent hydrogen bonds. Compounds are shown in stick representation. Residues are shown in thin sticks.

(PDB: 1XU9) forms similar hydrogen bond with the residue Tyr183 (Fig. 2A). Similar hydrogen bond also exists in the two crystal structures of the human 11β-HSD1 complexed with synthetic inhibitors (PDB: 2IRW and 2ILT).[23,24] Compounds **2** and **5** form hydrogen bonds with the N atom in Ala172. Besides, compound **2** forms two hydrogen bonds with Tyr177. The ligand in 1XU9 forms a hydrogen bond with the residue Tyr177, similar to compound **2**. Furthermore, in 1XU9,

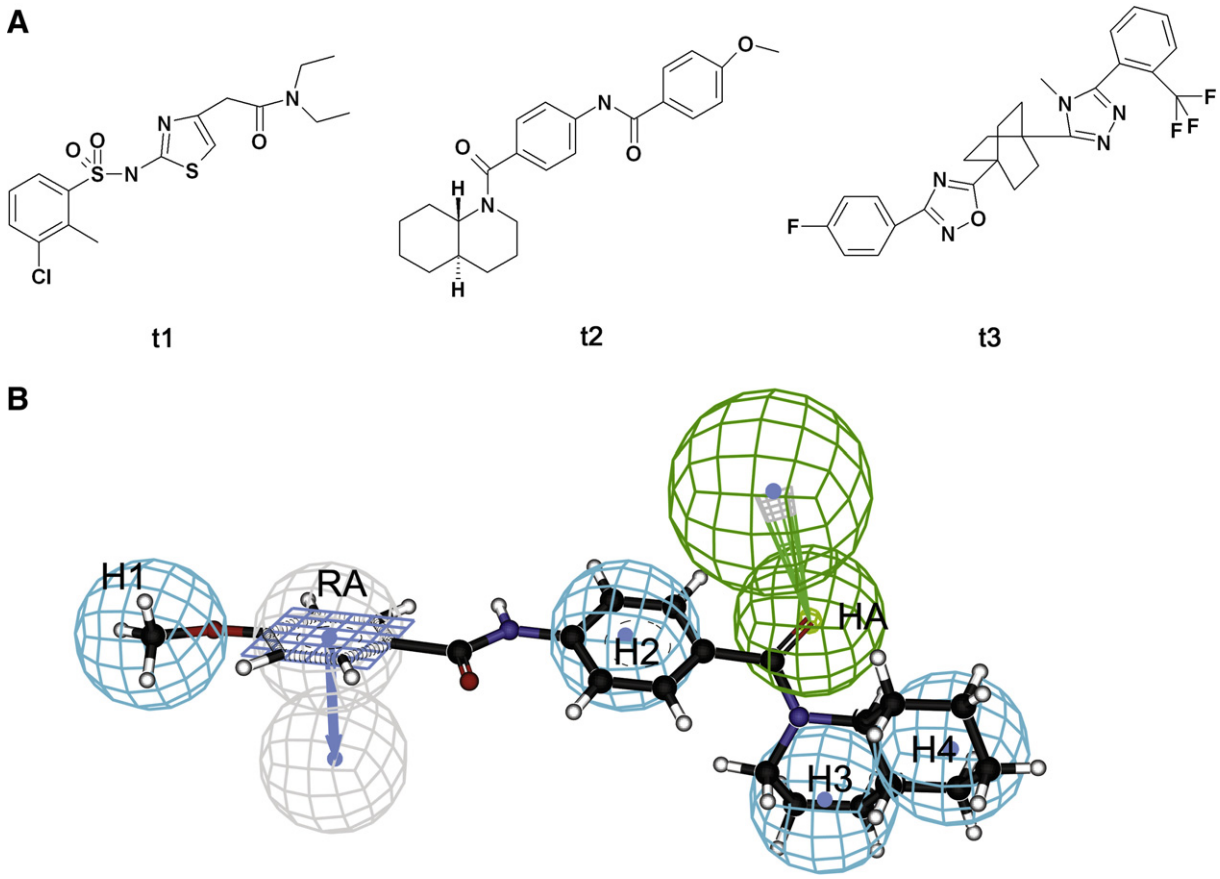

Figure 3. (A) Training compounds. (B) Compound **t2** fitted into Hypothesis 1. Hydrophobic features are shown in blue, Hydrogen-bond acceptor is shown in green, and ring aromatic feature is shown in gray. H1–H4, Hydrophobic features; HA, hydrogen-bond acceptor; RA, ring aromatic feature.

the ligand forms two hydrogen bonds with co-substrate $NADP^+$ (Fig. 2A). However, compounds **1**–**7** did not form any hydrogen bond with the co-substrate.

The ligand-based pharmacophore modeling method was also employed to discover active compounds that have the common features of known selective inhibitors. Based on their high bioactivity and structural diversity, three selective compounds (Fig. 3A)[25–27] were used as training set to build the pharmacophore model and identify the common features. The compounds were submitted to energy minimization and conformational analysis (maximum number of conformers = 250; generation type: best quality; energy range = 20 kcal/mol of minimum). The ConFirm program which is implemented in Catalyst (CATALYST 4.10.; Accelrys, Inc., San Diego, CA, 2005, <http://www.accelrys.com/>.) was used. Afterwards, the pharmacophore models for highly active 11β-HSD1 inhibitors were built by using the HipHop algorithm of Catalyst.[28,29] The best hypothesis (Hypothesis 1) as pharmacophore model was selected. As shown in Figure 3B, the model had four hydrophobic features, a hydrogen-bond acceptor, and a ring aromatic feature. A search among the 3000 compounds selected by using program DOCK 4.0 was performed with the Best Flexible Search mode and then the fit values were calculated. Compounds with high fit values were further filtered by druglikeness.

Finally, 100 compounds were selected and 82 of them were purchased. The other 18 compounds were out of stock. Again, the purchased compounds were evaluated by enzyme assay for their inhibition against the human and mouse 11β-HSD1. At concentration of 10 μM, the inhibitory rate of those compounds was in the range from 0% to 98.0%. Of the 82 compounds, seven showed high inhibition of human 11β-HSD1, while five showed high inhibition of mouse 11β-HSD1. Among the active compounds, seven compounds that were in enough reserves (compounds **10**–**16**) were put into concentration–response studies. Compounds **10**–**13** showed dose-dependent inhibition of human 11β-HSD1 with IC_{50} values ranging from 0.69 to 3.74 μM (Table 1 and Fig. 1). Compound **14** showed high inhibition of human 11β-HSD1, but dose-dependent inhibition was not observed. Compounds **12**, **13**, **15**, and **16** showed dose-dependent inhibition of mouse 11β-HSD1 with IC_{50} values ranging from 0.48 to 6.10 μM (Table 2 and Fig. 1).

In the following studies, mice were used as the animal models. Therefore, more attention was paid to compounds **2**, **8**, **9**, **12**, **13**, **15**, and **16** which showed high inhibition of mouse 11β-HSD1 (Table 2). In order to gain the highly selective inhibitors, these compounds were further tested for the inhibition against the mouse 11β-HSD2. Although these compounds showed high

Table 3. Inhibition of mouse 11β-HSD2 at 100 μM[a]

Compound	% Inhibition
2	3.4
8	3.7
9	2.2
12	0
13	9.1
15	0.8
16	1.6

[a] Values are averages of three determinations and deviation from the average is <10% of the average value.

inhibition against the mouse 11β-HSD1 with IC_{50} values ranging from 0.48 to 12.49 μM (Table 2), all compounds showed low inhibition against the mouse 11β-HSD2 at concentrations of 10 and 100 μM. Inhibition of mouse 11β-HSD2 at concentrations of 100 μM is listed in Table 3. It can be seen that all the compounds had excellent selectivity between the mouse 11β-HSD1 and 11β-HSD2.

In summary, by using docking and pharmacophore modeling, several compounds showing high inhibition against 11β-HSD1 have been discovered. Moreover, seven mouse 11β-HSD1 inhibitors show low inhibition of mouse 11β-HSD2 even at high concentration of 100 μM, which suggests they are selective 11β-HSD1 inhibitors. Additionally, the active compounds show large structural diversity and provide some new scaffolds for further study.

Acknowledgments

The authors thank Prof. Ping Jiang of Fudan university and Dr Yechun Xu of Weizmann Institute of Science for their help in revising English usage.
This work was supported by the 863 Hi-Tech Program (Grants 2006AA020602), the National Natural Science Foundation of China (Grants 30623008), and the New Drug Discovery Research Program of the Shanghai Institute of Materia Medica, Chinese Academy of Sciences (Grant 06G604P045).

References and notes

1. Arnaldi, G.; Angeli, A.; Atkinson, A. B.; Bertagna, X.; Cavagnini, F.; Chrousos, G. P.; Fava, G. A.; Findling, J. W.; Gaillard, R. C.; Grossman, A. B.; Kola, B.; Lacroix, A.; Mancini, T.; Mantero, F.; Newell-price, J.; Nieman, L. K.; Sonino, N.; Vance, M. L.; Giustina, A.; Boscaro, M. *J. Clin. Endocrinol. Metab.* **2003**, *88*, 5593.
2. Grundy, S. M.; Brewer, H. B., Jr.; Cleeman, J. I.; Smith, S. C., Jr.; Lenfant, C. *Circulation* **2004**, *109*, 433.
3. Inagaki, K.; Otsuka, F.; Miyoshi, T.; Watanabe, N.; Suzuki, J.; Ogura, T.; Makino, H. *Endocr. J.* **2004**, *51*, 201.
4. Kotelevitsev, Y.; Holmes, M. C.; Burchell, A.; Houston, P. M.; Schmoll, D.; Jamieson, P.; Best, R.; Brown, R.; Edwards, C. R. W.; Seckl, J. R.; Mullins, J. J. *Proc. Natl. Acad. Sci. U.S.A.* **1997**, *94*, 14924.
5. Masuzaki, H.; Paterson, J.; Shinyama, H.; Morton, N. M.; Mullins, J. J.; Seckl, J. R.; Flier, J. S. *Science* **2001**, *294*, 2166.
6. Kershaw, E. E.; Morton, N. M.; Dhillon, H.; Ramage, L.; Seckl, J. R.; Flier1, J. S. *Diabetes* **2005**, *54*, 1023.
7. Barf, T.; Williams, M. *Drugs Future* **2006**, *31*, 231.
8. Zimmet, P.; Alberti, K. G.; Shaw, J. *Nature* **2001**, *414*, 782.
9. Diederich, S.; Grossmann, C.; Hanke, B.; Quinkler, M.; Herrmann, M.; Bähr, V.; Oelkers, W. *Eur. J. Endocrinol.* **2000**, *142*, 200.
10. Alberts, P.; Nilsson, C.; Selén, G.; Engblom, L. O. M.; Edling, N. H. M.; Norling, S.; Klingström, G.; Larsson, C.; Forsgren, M.; Ashkzari, M.; Nilsson, C. E.; Fiedler, M.; Bergqvist, E.; Öhman, B.; Björkstrand, E.; Abrahmsén, L. B. *Endocrinology* **2003**, *144*, 4755.
11. Gu, X.; Dragovic, J.; Koo, G. C.; Koprak, S. L.; LeGrand, C.; Mundt, S. S.; Shah, K.; Springer, M. S.; Tan, E. Y.; Thieringer, R.; Hermanowski-Vosatka, A.; Zokian, H. J.; Balkovec, J. M.; Waddell, S. T. *Bioorg. Med. Chem. Lett.* **2007**, *17*, 2838.
12. Miguet, L.; Zhang, Z.; Barbier, M.; Grigorov, M. G. *J. Comput. Aided Mol. Des.* **2006**, *20*, 67.
13. Schuster, D.; Maurer, E. M.; Laggner, C.; Nashev, L. G.; Wilckens, T.; Langer, T.; Odermatt, A. *J. Med. Chem.* **2006**, *49*, 3454.
14. (a) Mundt, S.; Solly, K.; Thieringer, R.; Hermanowski-Vosatka, A. *Assay Drug Dev. Technol.* **2005**, *3*, 367; (b) The human and murine 11β-HSD1 and 11β-HSD2 enzyme were expressed in HEK-293 cells. Briefly, the sequences of human and murine 11β-HSD1 and 11β-HSD2 were obtained from the clones provided by NIH Mammalian Gene Collection. The pcDNA3-derived expression plasmids were constructed by inserting the sequence into the multiple clone site of pcDNA3 purchased from Invitrogen. HEK-293 cells were transfected with the pcDNA3-derived expression plasmid and selected by cultivation in presence of 700 μM g/ml of G-418. The microsomal fraction overexpressing 11β-HSD1 or 11β-HSD2 was prepared from the HEK-293 cells stably transfected with either 11β-HSD1 or 11β-HSD2 and used as the enzyme source for SPA. 11β-HSD1 containing microsomes was incubated with NADPH and [^{3}H]cortisone, then the product, [^{3}H]cortisol, was specifically captured by a monoclonal antibody coupled to protein A-coated SPA beads. The 11β-HSD2 screening was performed by incubating 11β-HSD2 microsomes with [^{3}H] cortisol and NAD^+ and monitoring substrate disappearance.
15. Hosfield, D. J.; Wu, Y.; Skene, R. J.; Hilger, M.; Jennings, A.; Snell, G. P.; Aertgeerts, K. *J. Biol. Chem.* **2005**, *280*, 4639.
16. Zhang, J.; Osslund, T. D.; Plant, M. H.; Clogston, C. L.; Nybo, R. E.; Xiong, F.; Delaney, J. M.; Jordan, S. *Biochemistry* **2005**, *44*, 6948.
17. Ewing, T.; Kuntz, I. D. *J. Comput. Chem.* **1997**, *18*, 1175.
18. Kuntz, I. D. *Science* **1992**, *257*, 1078.
19. Weiner, S. J.; Kollman, P. A.; Nguyen, D. T.; Case, D. A. *J. Comput. Chem.* **1986**, *7*, 230.
20. Gasteiger, J.; Marsili, M. *Tetrahedron* **1980**, *36*, 3219.
21. Zheng, S.; Luo, X.; Chen, G.; Zhu, W.; Shen, J.; Chen, K.; Jiang, H. *J. Chem. Inf. Model.* **2005**, *45*, 856.
22. Hult, M.; Shafqat, M.; Elleby, B.; Mitschke, D.; Svensson, S.; Forsgren, M.; Barf, T.; Vallgarda, J.; Abrahmsenb, L.; Oppermanna, U. *Mol. Cell. Endocrinol.* **2006**, *248*, 26.
23. Patel, J. R.; Shuai, Q.; Dinges, J.; Winn, M.; Pliushchev, M.; Fung, S.; Monzon, K.; Chiou, W.; Wang, J.; Pan, L.; Wagaw, S.; Engstrom, K.; Kerdesky, F. A.; Longenecker, K.; Judge, R.; Qin, W.; Imade, H. M.; Stolarik, D.; Beno, D. W.; Brune, M.; Chovan, L. E.; Sham, H. L.; Jacobson, P.; Link, J. T. *Bioorg. Med. Chem. Lett.* **2007**, *17*, 750.
24. Sorensen, B.; Winn, M.; Rohde, J.; Shuai, Q.; Wang, J.; Fung, S.; Monzon, K.; Chiou, W.; Stolarik, D.; Imade, H.;

Pan, L.; Deng, X.; Chovan, L.; Longenecker, K.; Judge, R.; Qin, W.; Brune, M.; Camp, H.; Frevert, E. U.; Jacobson, P.; Link, J. T.. *Bioorg. Med. Chem. Lett.* **2007**, *17*, 527.
25. Barf, T.; Vallgårda, J.; Emond, R.; Häggström, C.; Kurz, G.; Nygren, A.; Larwood, V.; Mosialou, E.; Axelsson, K.; Olsson, R.; Engblom, L.; Edling, N.; Rönquist-Nii, Y.; Öhman, B.; Alberts, P.; Abrahmsén, L. *J. Med. Chem.* **2002**, *45*, 3813.
26. Coppola, G. M.; Kukkola, P. J.; Stanton, J. L.; Neubert, A. D.; Marcopulos, N.; Bilci, N. A.; Wang, H.; Tomaselli, H. C.; Tan, J.; Aicher, T. D.; Knorr, D. C.; Jeng, A. Y.; Dardik, B.; Chatelain, R. E. *J. Med. Chem.* **2005**, *48*, 6696.
27. Gu, X.; Dragovic, J.; Koo, G. C.; Koprak, S. L.; LeGrand, C.; Mundt, S. S.; Shah, K.; Springer, M. S.; Tan, E. Y.; Thieringer, R.; Hermanowski-Vosatka, A.; Zokian, H. J.; Balkovec, J. M.; Waddell, S. T. *Bioorg. Med. Chem. Lett.* **2005**, *15*, 5266.
28. Barnum, D.; Greene, J.; Smellie, A.; Sprague, P. *J. Chem. Inf. Comput. Sci.* **1996**, *36*, 536.
29. Clement, O. O.; Mehl, A. T. *Pharmacophore Perception, Development, and Use in Drug Design*; International University Line: La Jolla, CA, 2000, pp. 69–84.